

# Solid-state and Solution-state NMR Studies of the Chlorophosphane (2,6-(CF<sub>3</sub>)<sub>2</sub>C<sub>6</sub>H<sub>3</sub>)(2,4-(CF<sub>3</sub>)<sub>2</sub>C<sub>6</sub>H<sub>3</sub>)PCl, (ArArPCl), and its Crystal Structure at 150 K

Andrei S. Batsanov,<sup>[a]</sup> Stephanie M. Cornet,<sup>[a]</sup> Lindsey A. Crowe,<sup>[a]</sup> Keith B. Dillon,<sup>[a]</sup> Robin K. Harris,<sup>\*[a]</sup> Paul Hazendonk,<sup>[a]</sup> and Mark D. Roden<sup>[a]</sup>

**Keywords:** NMR spectroscopy / Structure elucidation / Phosphanes / Configuration determination

The title compound has been synthesised, and characterised by multinuclear magnetic resonance spectroscopy, both in solution and in the solid state. The bandshapes of variable-temperature solution-state <sup>19</sup>F NMR spectra have been iteratively fitted to obtain information on the kinetics of rotation about the PC bond for one of the aryl groups, and values for the enthalpy and entropy of activation of the process have been derived. Magic-angle spinning NMR techniques have been extensively applied to the solid, using <sup>19</sup>F, <sup>31</sup>P and <sup>13</sup>C nuclei. Triple-channel methods and different magnetic field strengths have been employed to yield a range of complementary information. Heteronuclear interactions and intramolecular motions have been investigated. Bandshapes arising from (P, Cl) residual dipolar coupling have been analysed. Satisfactory agreement is found between experimental spectra and those simulated with estimated values of the parameters involved, and it is confirmed that the electric field gradient at chlorine is co-axial with the PCl bond. The sign of the isotropic (PCl) indirect coupling constant is obtained for the first time and is shown to be negative. The crystal structure of the compound at 150K confirms the presence of two different aromatic residues, as deduced from the spectroscopic studies.

and to investigate the interaction between phosphorus and the quadrupolar chlorine nucleus, as shown by residual dipolar splitting.

## Introduction

The novel compound 2,6-bis(trifluoromethyl)phenyl-2,4-bis(trifluoromethyl)phenyl-chlorophosphane (**1**) has been synthesised as part of a continuing study of low-coordinate phosphorus compounds containing bulky electron-withdrawing aromatic groups.<sup>[18]</sup> The formation of this compound with different bis(trifluoromethyl)phenyl groups arises (Exp. Section) because 1,5-bis(trifluoromethyl)benzene can be lithiated by butyllithium in two different positions: Either *ortho* to both CF<sub>3</sub> groups, giving a 2,6-bis(trifluoromethyl)phenyl-lithio derivative, or *ortho* to one of the CF<sub>3</sub> groups only, yielding the analogous 2,4-substituted compound. These groups are designated Ar and Ar' respectively herein. On treatment with PCl<sub>3</sub>, both of the dichlorophosphanes are obtained, with the 2,6 derivative (Ar) present in the larger amount. The isomers can be readily distinguished by their <sup>31</sup>P and <sup>19</sup>F solution-state spectra. The solid disubstituted product isolated from the reaction mixture was shown to be the title compound ArArPCl (Figure 1), firstly by solution-state NMR and secondly by extensive (<sup>31</sup>P, <sup>19</sup>F and <sup>13</sup>C) solid-state NMR investigations. Its structure was eventually determined by single-crystal X-ray diffraction at 150K. Variable-temperature solution-state <sup>19</sup>F NMR spectroscopy was used to determine the enthalpy and entropy of activation for internal rotation about the PC bond of the Ar group. The aims of the solid-state NMR experiments were to gain further structural information,

and to investigate the interaction between phosphorus and the quadrupolar chlorine nucleus, as shown by residual dipolar splitting.

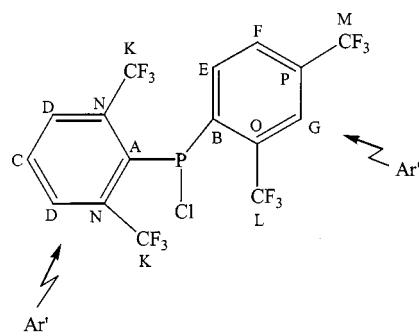


Figure 1. Lettering scheme for carbon atoms in ArArPCl (**1**)

A major feature of interest in the solid-state NMR spectrum of **1** is the bandshape of the <sup>31</sup>P resonance. Indirect isotropic (PCl) coupling should split the NMR signal of <sup>31</sup>P bonded to a single chlorine into a quadruplet of lines of equal spacing and intensity. In the solid state, dipolar coupling may also come into play; however, such coupling between two spin 1/2 nuclei is generally eliminated by MAS if the spin rate is fast enough. In the case of coupling to a quadrupolar nucleus, however, this may not be true and, although MAS will cause partial averaging, the spin 1/2 spectrum may retain a residual dipolar splitting, with powder bandshapes involved for each of the quadruplet lines mentioned above. Such effects have been fully discussed in many articles and reviews.<sup>[9]</sup> Most examples refer to <sup>13</sup>C<sup>14</sup>N

<sup>[a]</sup> Chemistry Department, University of Durham, South Road, Durham, DH1 3LE, UK Fax: (internat.) +44-191/386-1127 E-mail: r.k.harris@durham.ac.uk

interactions, but such effects have been seen<sup>[10]</sup> for the P/Cl pair in phosphonitrile chloride cyclic trimer. The case of  $\text{PCl}_5$  has also been studied, and the effect on the  $^{31}\text{P}$  spectrum of such residual dipolar coupling (RDC) to the four and six chlorines of the two counter-ions investigated (*AUTHOR: But  $\text{PCl}_5$  doesn't have any counter-ions. Please rephrase this sentence*).<sup>[11]</sup> At high temperature, however, both phosphorus environments give rise to sharp singlets because of fast isotropic reorientation and/or short spin-lattice relaxation times of the chlorine nuclei (self decoupling). Isotropic indirect (scalar) effects, when these are present, would only be affected by fast spin-lattice relaxation.

Provided the relevant quadrupole coupling constant,  $= e^2qQ/h$ , is small compared to the Larmor frequency of the quadrupolar spin, the residual dipolar splitting can be treated by perturbation theory.<sup>[9]</sup> In such a situation the outer pair of lines in the  $^{31}\text{P}$  spectrum influenced by isotropic indirect coupling to a chlorine nucleus will be shifted according to Equation(1):

$$\Delta = -\frac{3}{10} \chi^2 D / \nu_{\text{Cl}} \quad (1)$$

where  $D$  is the (PCl) dipolar coupling constant and  $\nu_{\text{Cl}}$  is the Larmor frequency of the chlorine nuclei. The inner pair of lines move by the same amount but in the opposite direction. In these cases it is often assumed that the electric field gradient tensor,  $q$ , is axially symmetric and that  $q$  and  $D$  (the dipolar tensor) are coaxial, but this is not necessarily true. A further common assumption is that the indirect coupling anisotropy,  $J$ , is negligible. Otherwise,  $D$  must be replaced by  $D = D/J/3$ , though even this assumes that  $J$  is axially symmetric and that  $D$  and  $J$  are coaxial. However, these simple situations are not necessarily the case for the P/Cl nuclear pair, so that use of the full Hamiltonian may be required.

The interactions between phosphorus and chlorine may, in principle, be complicated by the presence of the two different spin 3/2 isotopes for chlorine,  $^{35}\text{Cl}$  and  $^{37}\text{Cl}$ . However, due to their differing natural abundances and similar nuclear properties, it can be expected that the separate effects will not be resolved, given the observed linewidths. In simulations both isotopes can be accounted for.

## Results and Discussion

### Solution-State NMR Measurements

The molecular structure of the title compound was first established by solution-state NMR spectroscopy. The  $^{31}\text{P}$  spectrum (for a solution in  $\text{CH}_2\text{Cl}_2/\text{CDCl}_3$ ) consists of a complex multiplet at  $\delta = 67.3$ . The  $^{19}\text{F}$  spectrum (obtained for a  $[\text{D}_8]\text{toluene}$  solution) was expected to be composed of two doublets, one having double intensity (from the Ar group), and one singlet (in principle a doublet but with  $^6J_{\text{PF}}$  negligibly small). At ambient probe temperature, however, a doublet at  $\delta = 58.9$  ( $^4J_{\text{PF}} = 58.3\text{Hz}$ ), and two singlets (a

broad double-intensity line at  $\delta = 55$  and a sharp peak at  $\delta = 63.6$ ) were observed. At 98 C, the broad signal was resolved into the expected doublet [ $\delta = 54.9$  ( $^4J_{\text{PF}} = 41.7\text{Hz}$ )], demonstrating that rotation of the Ar group about the PC bond is fast enough on the NMR timescale for the two  $\text{CF}_3$  groups to become equivalent. At 90 C, however, two doublets and two singlets were detected (Figure2).

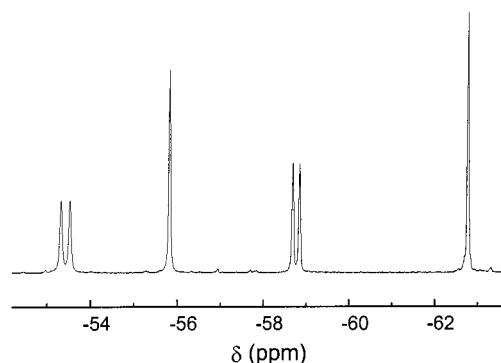


Figure 2. Fluorine-19 spectrum at 376.35 MHz and 90 C of a solution of  $\text{ArAr}^*\text{PCl}$  in  $[\text{D}_8]\text{toluene}$ ; the high-frequency doublet and the high-frequency singlet are assigned to the Ar group and are the resonances which broaden and coalesce at higher temperatures; spectrometer operating conditions: pulse angle 34.8, 16 transients, recycle delay 4.0 s

The doublet and singlet assigned to the Ar group were at virtually identical positions to those at room temperature ( $\delta = 58.8$  and  $62.8$ , respectively), suggesting either that rotation about the PAr bond is rapid on the NMR timescale even at low temperature or that there is a single fixed conformation about the PAr bond. For the Ar moiety, a doublet at  $\delta = 53.4$  ( $^4J_{\text{PF}} = 76.7\text{Hz}$ ) and a singlet at  $\delta = 55.8$  were found (consistent with the average  $\delta$  and  $J$  observed at +98 C). We believe that the values of  $^4J_{\text{PF}}$  in systems involving ArP or ArP linkages may contain a strong contribution from through-space effects. Therefore, this result implies that not only are the two  $\text{CF}_3$  groups of Ar inequivalent at 83 C, but also that one of them may be appreciably further away from the phosphorus atom. This was subsequently confirmed by the crystal structure, determined at 123 C (see below).  $^{19}\text{F}$  NMR spectroscopic data are summarised in Table1.

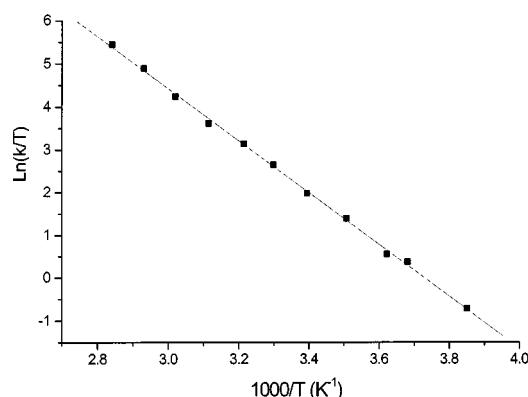
The Ar group rotation about the PC bond was investigated in detail by bandshape fitting for 12 temperatures between 15 C and 90 C on the basis of two-site equal-population mutual exchange. The coupling to  $^{31}\text{P}$  involves summing the intensity of two such exchange pairs, with equal intensity but slightly different effective chemical shifts for one of the sites. Figure3 shows the Eyring plot for the exchange. The resulting thermodynamic parameters are:  $H = 51.0 \pm 0.6 \text{ kJ mol}^{-1}$  and  $S = 8 \pm 3 \text{ J K}^{-1} \text{ mol}^{-1}$ , the errors quoted representing only the statistics of the linear fit.

The  $^{13}\text{C}\{^1\text{H}\}$  NMR spectrum was also recorded for a toluene/ $\text{CDCl}_3$  solution at ambient temperature. Probable assignments (see Figure1 for the notation) are shown in Table2, though some of these are necessarily tentative. In particular the signals from the carbons to which the  $\text{CF}_3$

Table 1. Comparison of fluorine chemical shift data in different situations for compound **1**

	Assignment	$\delta/\text{ppmAr}$	$\delta/\text{ppmAr}$	$\delta/\text{ppmAr}$	$\delta/\text{ppmAr (para)}$	Average linewidth/Hz
Solution	high temp. 98 C	54.9 <sup>[a]</sup>		58.8 <sup>[b]</sup>	64.0	
ambient temp. 22 C	55 <sup>[c]</sup>		58.9 <sup>[d]</sup>	63.6		
low temp. 83 C	53.4 <sup>[e]</sup>	55.8	58.8 <sup>[f]</sup>	62.8		
Solid	high temp. 50 C	54.1	57.7	59.9	65.3	568
ambient temp.	54.3	58.0	60.3	65.5	597	
low temp. 120 C	55.1	57.9, <sup>[g]</sup> 59.2 <sup>[g]</sup>	61.4	66.6	680	

<sup>[a]</sup> Doublet (double intensity).  $^4J_{\text{PF}} = 41.7\text{Hz}$ . <sup>[b]</sup> Doublet.  $^4J_{\text{PF}} = 56.8\text{Hz}$ . <sup>[c]</sup> Broad, double intensity. <sup>[d]</sup> Doublet.  $^4J_{\text{PF}} = 58.3\text{Hz}$ . <sup>[e]</sup> Doublet.  $^4J_{\text{PF}} = 76.7\text{Hz}$ . <sup>[f]</sup> Doublet.  $^4J_{\text{PF}} = 59.5\text{Hz}$ . <sup>[g]</sup> Low intensity.

Figure 3. Eyring plot for the exchange of the CF<sub>3</sub> groups of the Ar moiety in ArArPCl by internal rotation about the PC bond in the solution state

groups were attached were of low intensity (presumably because the recycle delay used to secure good S/N for the other peaks was inadequate for relaxation of these carbons), and in a similar region to other signals. The presence of two distinct resonances for carbons *ipso* to phosphorus confirms the asymmetric nature of the title compound, as does the observation of three different CF<sub>3</sub> signals, one of double intensity.<sup>2</sup>

Table 2. Assignments for the solution-state <sup>13</sup>C spectrum of **1**

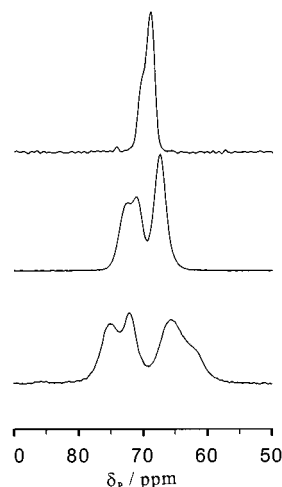
Carbon <sup>[a]</sup>	$\delta/\text{ppm}$	$J/\text{Hz}^{[b]}$
A	137.6	d, $^1J_{\text{PC}} 67.9$
B	136.7	d, $^1J_{\text{PC}} 84.0$
C	132.11 <sup>[c]</sup>	s
D	131.1	s (broad, double intensity)
E	134.2	d, $^2J_{\text{PC}} 8.7$
F	128.0	d, $^2J_{\text{PC}} 3.4$
G	123.7	m, $^3J_{\text{FC}} 5.0$
K	123.18 <sup>[c]</sup>	q, $^1J_{\text{FC}} 275.8$ (double intensity)
L	123.24 <sup>[c]</sup>	qd, $^1J_{\text{FC}} 275.5$ , $^3J_{\text{PC}} 3.4$
M	123.1	q, $^1J_{\text{FC}} 272.6$
N	132.06 <sup>[c]</sup>	m
O	132.3	m
P	131.8	m

<sup>[a]</sup> See Figure 1. <sup>[b]</sup> Only the magnitudes of coupling constants were obtained, not the signs. <sup>[c]</sup> Although the absolute accuracy of the chemical shifts is only quoted to one decimal place, a further digit is given when two signals are very close but resolved.

#### Residual Dipolar Coupling Between <sup>31</sup>P and <sup>35/37</sup>Cl

A single phosphorus environment for **1** in the solid state is indicated by the <sup>31</sup>P CPMAS spectrum, as expected from

the fact that the crystallographic asymmetric unit is one molecule (see below). However, the signal was split into four lines at the lowest applied magnetic field used due to the effect of the adjacent chlorine (Figure 4, lowest trace). The apparent chemical shifts of these lines were  $\delta = 75$ , 72, 66 and 62 for the 200MHz spectrometer, the last two not being completely resolved (though a shoulder was easily observable). The four shifts were obtained by deconvolution using the Spinsight software.<sup>[12]</sup>

Figure 4. Phosphorus-31 {<sup>1</sup>H} spectra of solid ArArPCl; centreband region only; spectral frequencies (top to bottom) 242.95MHz, 121.42MHz, 81.02MHz; cross-polarisation from protons; contact time 9 ms, recycle delay 5 s, number of acquisitions between 150 and 450

The nature of the splitting was identified by running spectra at different field strengths, namely on the 200, 300 and 600MHz (proton) spectrometers (Figure 4). The splitting decreased on both a frequency and a ppm scale, confirming that there is a single phosphorus resonance affected by residual dipolar coupling to the adjacent quadrupolar chlorine. Such coupling can be contrasted with the cases of isotropic (indirect) coupling or crystallographic splittings, which decrease in ppm and increase in Hz, respectively, on going to higher magnetic field strength. Where all four lines can be seen (for the CMX 200 spectrometer), the separations of the lines are 228, 602 and 287Hz (from high to low frequency). The first two splittings were still resolved at 121.42MHz and are 188 and 449Hz respectively. At the highest field no splitting was observed within the linewidth

of 650Hz (the separation of a high-frequency shoulder peak from the signal maximum was approximately 350Hz). At each field the individual bandshapes did not show any significant changes over the spinning sideband manifold. The value of the isotropic coupling constant,  $J_{\text{PCl}}$ , is likely to be around 100130Hz in magnitude,<sup>[13]</sup> so it is not surprising that no splitting from this cause is resolved at the highest field. At 121.42MHz the appearance of the spectrum approached that of a doublet (i.e.  $J_{\text{PCl}}$  not significantly effective),<sup>[14]</sup> whereas at lower field there was further perturbation, producing a more complex multiplet.

From ab initio calculations using Gaussian94,<sup>[15]</sup> the electric field gradient (EFG) of the quadrupolar chlorine nucleus can be estimated. For this computation the full molecular structure was used, and the calculations to give the NMR parameters also included a structural energy minimisation. Results were converted to an appropriate axis system within a Mathcad worksheet.  $q$  is calculated by multiplying  $q$  (obtained in atomic units as the largest component of the electric field gradient from a HartreeFock approximation using the 631g\* basis set) by  $2.3495 \times 10^{36} \text{ C J}^{-1} \text{ s}^{-1}$ . Values of  $q$  of 55 and 44MHz were calculated for  $^{35}\text{Cl}$  and  $^{37}\text{Cl}$  respectively, with the major EFG axis approximately along the PCl bond and a low value (but nonzero) for the asymmetry parameter. NQR frequencies of magnitude 25.5, 25.7 and 26.3MHz have been reported for  $\text{Et}_2\text{PCl}$ ,  $\text{Bu}_2\text{PCl}$  and  $(\text{C}_6\text{H}_5)_2\text{PCl}$ , respectively.<sup>[16]</sup> These represent the magnitude of  $1/2e^2Qq/h$  (i.e.  $1/2$ ) if the asymmetry parameter is zero, and therefore show that the values used in the calculations for the compound studied here are reasonable. The value of  $D$  may be obtained for **1** from the known PCl distance of 2.0608(6) Å (this work). For  $^{31}\text{P}$ ,  $^{35}\text{Cl}$  the result is  $D = 662\text{Hz}$ , whereas for  $^{31}\text{P}$ ,  $^{37}\text{Cl}$  it is 551Hz. Thus values of  $D$ , the parameter defining the second-order effects under perturbation theory, may be calculated, assuming  $D = D$  (i.e. ignoring  $J$ ). These results are given in Table 3. The predicted values are of the correct order of magnitude to account for the observed splittings, but a reasonable fit to the spectra at the different fields cannot be obtained, so a more accurate calculation is required.

tween the PCl interatomic distance and the EFG axis). A nonzero value of the isotropic scalar coupling,  $J_{\text{PCl}}$ , can also be incorporated. The values of  $J$  used were: 55MHz for the  $^{35}\text{Cl}$  isotope and 44MHz for  $^{37}\text{Cl}$  (vide supra). The magnitude of  $J(^{31}\text{P}, ^{35}\text{Cl})$  was set to a little lower than the literature values for related systems,<sup>13</sup> i.e. to 100Hz (which implies that  $J(^{31}\text{P}, ^{37}\text{Cl})$  is 83Hz), since this seemed to yield a slight improvement in the fitting, and  $D$  was given the value calculated from the crystal structure (therefore assuming a negligible value of the anisotropy in  $J$ ). As indicated before, a splitting of ca. 100Hz is significantly less than the observed linewidths and so will not be resolved, but it may, however, contribute to the distortion of the multiplet pattern. The relevant parameters were varied in the simulation and fitting by eye attempted. Altering  $D$  to include a possible anisotropy in  $J_{\text{PCl}}$  would lead to a slight change in the total width of the whole pattern, but changing the value of  $D$  ( $D$ ) from 500 to 660Hz does not, in practice, have a significant effect on the simulated spectrum. A larger magnitude of  $J_{\text{PCl}}$  than 100Hz does lead to an increase in the outer splittings and a smaller value for the largest central splitting. However, changing the sign of  $J_{\text{PCl}}$  has a much more marked effect. Whereas a positive value led to substantial discrepancies between observed and simulated spectra, a negative value resulted in a good fit (see Figure 3 and 4) at both 81.02 and 121.42MHz. Several different angles were used (in the range 0 to 180) and the approximate splittings of the simulated bands compared to the experimental data. The best agreement at 81.02MHz was found with  $\alpha = 0$ , giving approximate splittings of 200, 670 and 300Hz measured between the centres of gravity of the simulated powder patterns involving  $^{35}\text{Cl}$  (experimental values are 228, 602 and 287Hz). If  $\alpha$  is increased to 20, the splittings move significantly away from the experimental values, giving four bands with more nearly equal separation. At higher values of  $\alpha$ , of around 90, the lines converge and the difference between the experimental and simulated spectra is obvious. Given that this system consists of a directly bonded spin-pair involving a monovalent quadrupolar nucleus, co-axiality of the EFG and the PCl bond is expected, so this result

Table 3. Theoretical parameters for the reduced P,Cl dipolar splittings observed for compound **1**

$^{31}\text{P}$ frequency/MHz	Isotope	D/Hz <sup>[a]</sup>	MHz	Hz	2Hz	Observed splitting/Hz <sup>[b]</sup>
81.02	$^{35}\text{Cl}$	662	55	557	1114	860
$^{37}\text{Cl}$	551	44	446	892		
121.42	$^{35}\text{Cl}$	662	55	372	744	560
$^{37}\text{Cl}$	551	44	297	594		
242.95	$^{35}\text{Cl}$	662	55	186	372	350
$^{37}\text{Cl}$	551	44	149	298		

<sup>[a]</sup> Assuming  $r_{\text{PCl}} = 1.93 \text{ Å}$ . <sup>[b]</sup> Doublet splitting at the highest field, and approximate separation of the midpoints of the pairs of doublets at 81.02 and 121.42MHz.

Using a program based on the full Hamiltonian approach,<sup>[9,17]</sup> the bandshapes at 200 and 300MHz were simulated (Figure 5). This calculates the MAS spectrum of a spin 1/2 nucleus under the influence of a quadrupolar ( $I = 3/2$ ) spin, with the assumption of axial symmetry of the electric field gradient, but with variation allowed for the angle ( $\beta$ )

gives confidence in the methods used. The calculated splittings (for  $\beta = 0$ ) involving  $^{35}\text{Cl}$  at 121.42MHz are 270, 470 and 230Hz (compared with measured values 188 and 449Hz, the third splitting being unresolved in this experimental spectrum). At 242.95MHz, there is not sufficient resolution in the experimental spectrum to make any mean-



ingful comparison with the simulated lineshapes. However, the overall width of the lines shows reasonable agreement with the width of the unresolved doublet.

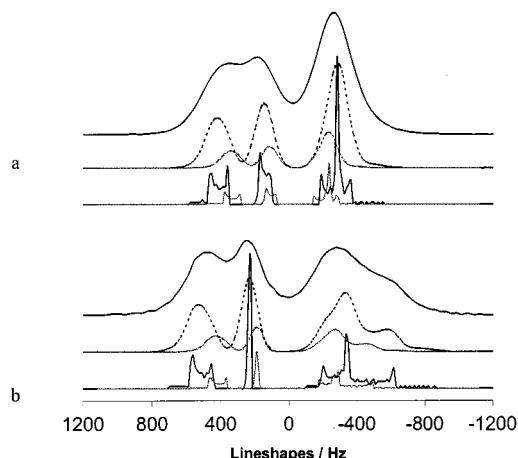


Figure 5. Experimental (upper solid lines) and simulated centreband shapes for the <sup>31</sup>P spectra of solid ArArPCl run at 121.42 MHz (a) and 81.02 MHz (b); the calculated powder bands are shown below for coupling to <sup>35</sup>Cl (black lines) and <sup>37</sup>Cl (grey lines) in the appropriate proportions, with  $J(^{31}\text{P}, ^{35}\text{Cl}) = 100\text{ Hz}$  and  $J(^{31}\text{P}, ^{37}\text{Cl}) = 83\text{ Hz}$ , respectively; the dotted lines represent the two simulated spectra, with a line broadening of 100 Hz

A value of slightly lower in magnitude (around 50 MHz) than that calculated by ab initio methods was found to be perhaps more appropriate for the most abundant isotope, <sup>35</sup>Cl. In this case the simulated bands are brought slightly more in line with the experimental data. With an even lower value of the intensity differences between calculated and experimental spectra become more significant. Perturbation theory makes it clear that the principal variable is the product  $D$ .

Figure 5 shows a comparison of the experimental and final simulated lineshapes. There is obviously significantly more broadening of the experimental lineshapes, but for ease of distinguishing the individual lines the simulation linewidth was kept low. The contribution from <sup>37</sup>Cl gives significantly different lineshapes to that from <sup>35</sup>Cl (see Figure 5). The simulated spectra were obtained by summing the two contributions in the appropriate proportions. After line broadening has been applied there are only minor discrepancies between observed and simulated spectra, so it is clear that the parameters used for the latter are close to their correct values. In particular, it is proved that isotropic  $J_{\text{PCl}}$  is negative (Figure 6). Because of the quadrupolar nature of the chlorine isotopes, very few values of this coupling constant have been reported, and this is the first determination of the sign.

Of course, there are still assumptions involved in the spectral simulation, especially axial symmetry in the EFG tensor, and there were limitations of not being able to optimise all the parameters by small increments because of the computational time involved in the calculation of each spectrum. This work represents the first time a <sup>31</sup>P reduced

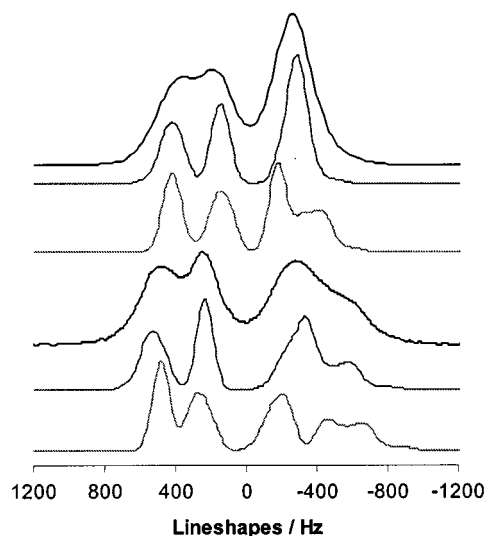


Figure 6. Centreband <sup>31</sup>P bands for solid ArArPCl at 121.42 MHz (top 3 spectra) and 81.02 MHz (bottom 3 spectra); for each trio of spectra the top one is as experimentally observed, the middle one is as simulated for  $J(^{35}\text{Cl}, ^{31}\text{P}) = 100\text{ Hz}$  and the bottom one as simulated for  $J(^{37}\text{Cl}, ^{31}\text{P}) = +100\text{ Hz}$ ; note that the simulations do not include a contribution from molecules containing the <sup>37</sup>Cl isotope

dipolar coupling pattern has been successfully simulated, including the first use of combined <sup>35</sup>Cl and <sup>37</sup>Cl effects.

#### Cross-Polarisation Experiments

Both <sup>19</sup>F and <sup>1</sup>H nuclei were used for polarisation transfer to phosphorus. All three nuclei are abundant in the sense that their natural isotopic proportion of the element is 99.9%. Therefore cross-polarisation dynamics are more complex than may appear at first sight. For instance, although results from a <sup>1</sup>H<sup>31</sup>P variable-contact-time experiment may in general be fitted to only two parameters (a rise time  $T_{\text{HP}}^{\text{eff}}$  and a decay time  $T_1^{\text{eff}}$ ) these cannot be simply related to the specific cross-polarisation time  $T_{\text{HP}}$  and single-nucleus  $T_1^{\text{H}}$  respectively. Instead, both measured parameters depend on  $T_{\text{CP}}$ ,  $T_1^{\text{H}}$  and  $T_1^{\text{P}}$ . A detailed analysis of this problem may be found in refs.<sup>[18,19]</sup> On the other hand, for compound **1**, phosphorus is chemically dilute in the sense that there is only one <sup>31</sup>P per molecule, which is likely to result in a long  $T_1^{\text{P}}$  (motional questions notwithstanding), as for the common case of <sup>13</sup>C. When the ratio of spins  $\gamma_{\text{YX}} = N_{\text{Y}}/N_{\text{X}}$  for a system involved in an XY CP experiment is low, deviations from simple behaviour are expected to be small. In the present case  $\rho_{\text{F}}$  is 1:12 and  $\rho_{\text{H}}$  is 1:6. It is found that for both <sup>19</sup>F<sup>31</sup>P and <sup>1</sup>H<sup>31</sup>P the rise of magnetisation during a variable contact time is substantially faster than the  $T_1$ -dependent decay. For <sup>19</sup>F to <sup>31</sup>P cross polarisation, both the TORQUE (TOneRhoQUEnching)<sup>[20]</sup> curve (for which the total constant spin-lock time was 10 ms) and the standard cross-polarisation experiment show an almost horizontal region at long spin-lock times. This implies that  $T_1^{\text{F}}$  and  $T_1^{\text{P}}$  are both long. The measured cross-polarisation time  $T_{\text{HP}}^{\text{eff}}$  is relatively short (ca. 0.5 ms) and  $T_1^{\text{eff}}$  is a lot longer than the maximum duration of spin-

lock pulse available from the amplifiers. It is therefore difficult to measure these accurately, but a value for  $T_1^F$  of approximately 100 ms was obtained from a  $^{19}\text{F}^{31}\text{P}$  CP experiment, with a variable pre-contact spin-lock time. The effective value of  $T_{\text{HP}}$  derived from  $^1\text{H}^{31}\text{P}$  cross polarisation is longer, at 3.5 ms, than  $T_{\text{FP}}^{\text{eff}}$ . In the  $^1\text{H}^{31}\text{P}$  experiment the TORQUE curve has a positive slope at long spin-lock time, suggesting<sup>[17,18]</sup>  $T_1^{\text{H}} > T_1^{\text{P}}$ , as expected.

#### Solid-State $^{19}\text{F}$ Spectra

High-resolution  $^{19}\text{F}$  spectroscopy of solids containing hydrogen as well as fluorine has been the subject of relatively few investigations to date because the proximity of  $^1\text{H}$  and  $^{19}\text{F}$  resonance frequencies requires a specialised probe to facilitate proton decoupling with sufficient frequency filtering. The present experiments provide evidence of the value of solid-state  $^{19}\text{F}$  NMR spectroscopy for structural characterisation when such problems are overcome.  $^{19}\text{F}$  spectra (Figure 7) of the solid powdered sample were obtained over the temperature range 120 C to +50 C.

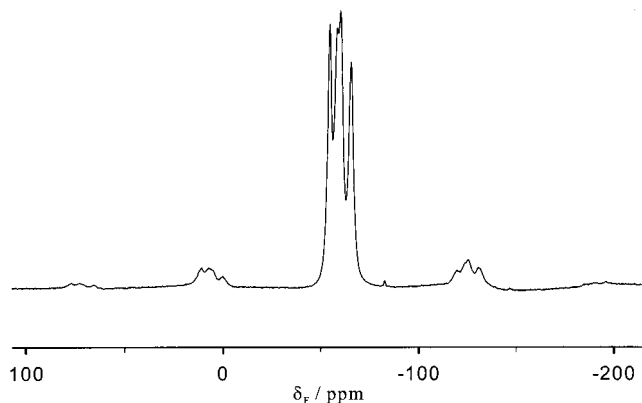


Figure 7. Fluorine-19 direct-polarisation spectrum of solid Ar-APCl; spectral frequency 188.3 MHz, recycle delay 2 s, number of acquisitions 400, spin rate 12 kHz

Throughout this range, the spectra show four peaks of approximately equal intensity within experimental error (considering the overlap of lines), with chemical shifts of  $\delta = 54, 58, 60,$  and  $65$ , although no splitting arising from  $^4J_{\text{PF}}$  was resolved because the linewidths are broader than in solution. These observations indicate that there are different environments for all four  $\text{CF}_3$  groups, indicating the lack of molecular symmetry and in conformity to the solution-state spectra. Rapid internal rotation will cause averaging of the positions, and therefore also of the chemical shifts of the three fluorines in each  $\text{CF}_3$  group. It is also observed that, in contrast to the solution state differences in splitting due to PF coupling between the four  $\text{CF}_3$  bands, there were no obvious variations in linewidths from deconvolution of the four peaks for the solid state, so only average values are quoted in Table 1. There was little change in the spectrum as the temperature was lowered, and the value of  $T_1^F$  remained relatively constant at around  $0.9 \pm 0.1$  s, within experimental error, from 20 down to 80 C, with a slightly

lower value of 0.6 s at ambient temperature (27 C). All four peaks showed small, similar trends in chemical shift to lower values as the temperature decreased, possibly arising from a variation in the referencing.

#### Solid-State $^{13}\text{C}$ Spectra

The  $^{13}\text{C}$  spectrum of the solid (with cross polarisation from protons, using a recycle delay of 5 s and a contact time of 8 ms) appears to consist of three peaks with chemical shifts  $\delta = 134, 133,$  and  $129$  (by deconvolution) (Figure 8). All these peaks were also observed in a dipolar dephasing experiment<sup>[21]</sup> in which only quaternary (or methyl) carbons remain. With an echo experiment run with identical conditions apart from the presence of the 50 s dephasing time, a subtraction of the normal and dipolar dephased spectra was made, resulting in a spectrum of protonated carbons only. In this case a broad underlying peak was observed with a maximum intensity at  $\delta = 134$ . By taking advantage of the different cross polarisation and decoupling combinations possible in a fluorinated molecule and the triple-channel HFX probe, further conclusions about the carbon spectrum can be made. The low-frequency peak increases significantly in intensity on application of cross polarisation from fluorine, as does that at the highest frequency, indicating proximity of these carbons to the  $\text{CF}_3$  groups. The lowest frequency peak also displays narrowing on application of fluorine decoupling. Although all these peaks appear in the aromatic  $^{13}\text{C}$  region, no peaks were observed in any other region of this spectrum. It is concluded that the  $\text{CF}_3$  resonances are also contained within this region. This result is supported by the solution-state spectrum described earlier, where all the relevant resonances lie between  $\delta = 138$  and  $123$ .

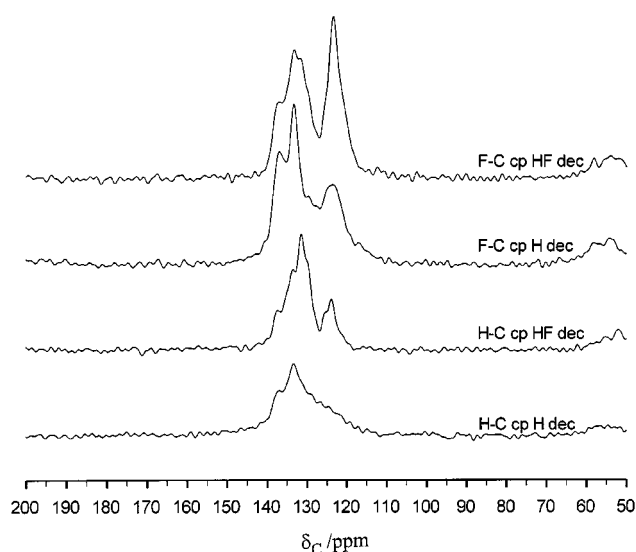


Figure 8. Solid-state  $^{13}\text{C}$  spectra at 50.33 MHz for compound **1** under various experimental regimes: cross polarisation, with contact time 7 ms, recycle delay 10 s, spin rate 4 kHz;  $^{19}\text{F}^{13}\text{C}$  CP and  $^1\text{H}^{13}\text{C}$  CP used 280 and 64 acquisitions, respectively

*X-ray Structure of ArArPCl*

The crystal structure of the title compound at 150K is shown in Figure 9, together with selected bond lengths and angles; according to the October 1999 release of the Cambridge Structural Database (CSD),<sup>[22]</sup> this is the first Ar<sub>2</sub>PCl compound to be structurally characterised. The structure shows some interesting features arising from steric and intramolecular interactions. The three covalent bonds to the P atom have a pyramidal configuration, complemented by two relatively short intramolecular contacts PF(1) at 2.890(1) Å and PF(8) at 2.897(1) Å, approximately in *trans* positions to covalent bonds [angles C(9)PF(1) = 172.45(5); CIPF(8) = 163.08(3)]. These contacts are shorter than the sums of the empirical van der Waals radii<sup>[23]</sup> of P (1.91 Å) and F (1.40 Å), as well as the theoretical ones (estimated as 2.05 and 1.42 Å respectively).<sup>[24]</sup> As deduced from the <sup>19</sup>F solution-state NMR spectra at low temperatures, there are marked differences in the fluorine-to-phosphorus distances for the two *ortho* CF<sub>3</sub> groups in the Ar moiety. The calculated distances to F(5) and F(6) are 3.68 and 3.25 Å, respectively, compared with 2.89 Å to F(1) or F(2). Rapid rotation of each of these groups about the CCF<sub>3</sub> bonds is expected at higher temperatures, but the average PF distance will still be longer to one CF<sub>3</sub> group than the other. These observations allow the <sup>19</sup>F signal at 83 °C at  $\nu_F = 53.4$  to be assigned to F(1,2,3), assuming there is a significant through-space contribution to <sup>4</sup>J<sub>PF</sub> (see above). The short PF(8) distance is then consistent with the existence of a moderately large <sup>4</sup>J<sub>[P,F(8)]</sub>. Such conclusions assume the structure of the molecule in solution is very similar to that in the crystalline solid. There is a possible hydrogen bond between the chlorine and the *ortho* hydrogen of the Ar group, at a calculated distance of 2.52 Å. This H-bond lies in the same plane as that of the aromatic ring of Ar, and may thus play an important role in determining the conformation of the compound. Because of the influence of the bulky CF<sub>3</sub> groups, the two aromatic rings form a dihedral angle of 94°.

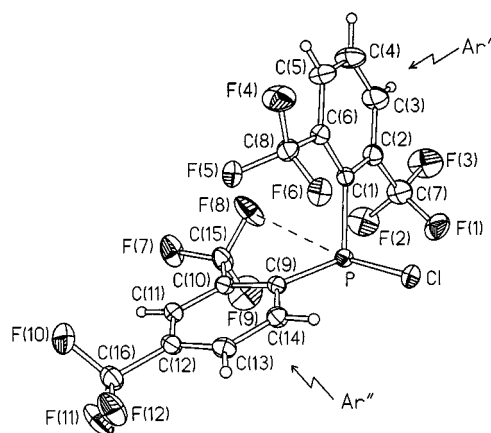
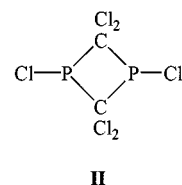


Figure 9. Molecular structure of **1**, showing 50% thermal ellipsoids; selected bond lengths (Å) and angles (°): PCl 2.061(1), PC(1) 1.875(1), PC(9) 1.852(1); CIPC(1) 100.23(4), CIPC(9) 102.10(5), C(1)PC(9) 109.23(6)

The PCl bond of 2.061(1) Å is relatively short; in eleven previously reported R<sub>2</sub>PCl (where at least one of the R groups is alkyl) structures (CSD) this distance varies from 2.06 to 2.35 Å, with the exception of the four-membered ring compound **II**, where it is reduced to between 2.01 and 2.03 Å.<sup>[25]</sup> The PCl distance is clearly sensitive to electronic effects from other groups bonded to phosphorus, and its shortening here can be attributed to the electron-withdrawing properties of the CF<sub>3</sub> groups on the aromatic rings.



## Experimental Section

**Synthesis of AArPCl:** *n*BuLi (57 mL of a 1.6 M solution in hexanes, 91.2mmol) was added dropwise over 10 minutes to a solution of 1,3,5-tris(trifluoromethyl)benzene (ArH) (20.03g, 94mmol) in ether (200 mL) at 78 °C. The solution was allowed to warm to room temperature and left stirring for four hours. A dark brown solution containing ArLi and ArLi was formed. It was added dropwise at 78 °C to a solution of PCl<sub>3</sub> (16 mL, 25.2g, 162mmol) in ether (100 mL) over 10 minutes. The mixture was allowed to warm to room temperature, and a precipitate of LiCl slowly formed. This was filtered off, and the solvent and excess PCl<sub>3</sub> removed from the filtrate in vacuo, leaving a brown intractable oil. A mixture of ArPCl<sub>2</sub> and ArPCl<sub>2</sub> (9.46g, 42%) was obtained by distillation at 45 and 0.01 Torr. Further distillation led to ArArPCl at 93 °C (0.01 Torr); yield (based on ArH) 7.45g, 26%. The compound was purified by recrystallisation from hexanes. C<sub>16</sub>H<sub>6</sub>ClF<sub>12</sub>P (492.63): calcd. C 39.01, H 1.23; found C 38.94, H 1.24.

**Solution-State NMR Spectroscopy:** Solution-state NMR spectra were recorded in 5mm o.d. sample tubes on a Varian VXR 400 Fourier-transform spectrometer, operating at 100.57 (<sup>13</sup>C), 161.91 (<sup>31</sup>P) and 376.35 (<sup>19</sup>F) MHz. Internal reference signals of TMS or CFCl<sub>3</sub> were used for <sup>13</sup>C and <sup>19</sup>F spectra, respectively, while an external reference of 85% H<sub>3</sub>PO<sub>4</sub> was employed for all <sup>31</sup>P spectra. For the <sup>13</sup>C spectrum, 12824 FIDs were accumulated, using pulse angle 48.7 and recycle delay 3 s. The corresponding values for the <sup>19</sup>F spectra were 16, 34.8 and 4 s, respectively, whereas those for the <sup>31</sup>P spectra were 492, 36 and 3 s, respectively. Fluorine-19 bandshape fitting for the exchange process was carried out using an in-house computer program involving a complete Liouville treatment (including exchange rates, chemical shifts and transverse relaxation rates as variables). This program was developed in the MATLAB environment. Iteration to the bandshape was optimised to 2°. Temperatures were calibrated using the chemical shift differences between the CH<sub>3</sub> and OH resonances of methanol (for temperatures below ambient) and between the CH<sub>2</sub> and OH resonances of glycol (for high temperatures). The standard Varian hardware was employed for temperature control.

**Solid-state NMR Spectroscopy:** Because the sample could be subject to possible decomposition if exposed to moist air, it was sealed in a small plastic insert, which then fitted tightly into the rotors used.



The spectrometers used for solid-state NMR were: Chemagnetics CMX200, Varian Unity Plus 300, and Chemagnetics Infinity 600. Most of the results were obtained on the lowest field spectrometer with which three main probes were used. The diameters of the rotors are: HX and HFX probes, 7.5mm, and HF probe, 4mm. These allow almost any combination of observation, cross polarisation and decoupling to be carried out, with the use of appropriate filters. Recycle delays were initially determined by variable delay-time experiments and checked by measurement of  $T_1^H$  where appropriate. A recycle delay of 5 s and a 1 ms contact time were found to be optimum for the  $^{31}\text{P}$  spectra. For cross-polarisation experiments, optimum contact times were found by arraying this parameter and choosing that with the greatest signal intensity. Spin rates used were generally 46kHz with the 7.5mm rotors and 1015kHz for the 4mm rotor. However, the small (3.2mm diameter) rotor system used with the Chemagnetics 600 spectrometer meant that a speed of 16.5kHz was easily attained. The frequencies of the individual nuclei on the three spectrometers are: (i) for the Chemagnetics CMX200:  $^{31}\text{P}$ , 81.02MHz;  $^{13}\text{C}$ , 50.33MHz;  $^{19}\text{F}$ , 188.29MHz;  $^1\text{H}$  200.13MHz, (ii) for the Varian Unity Plus 300:  $^{31}\text{P}$ , 121.42MHz;  $^{13}\text{C}$ , 75.43MHz;  $^1\text{H}$  299.95MHz, and (iii) for the Chemagnetics Infinity 600:  $^{31}\text{P}$ , 242.95MHz;  $^1\text{H}$  600.13MHz.

Referencing was done by replacement, setting the chemical shift scales as follows using the compounds named:  $^{31}\text{P}$ ,  $\text{CaHPO}_4$  set to = 1.2 (w.r.t. the signal for 85%  $\text{H}_3\text{PO}_4$  at zero ppm, though this primary standard was used directly as the reference on the 300MHz instrument);  $^{19}\text{F}$ ,  $\text{C}_6\text{F}_6$  set to = 166.4 w.r.t. the signal for  $\text{CFCl}_3$ ;  $^{13}\text{C}$ , high-frequency peak of adamantane set to = 38.4 w.r.t. the signal for  $(\text{CH}_3)_4\text{Si}$ . Fluorine shifts are corrected for the BlochSiegert effect<sup>[26]</sup> at ambient probe temperature by recording the reference  $^{19}\text{F}$  resonance with high-power irradiation at the proton frequency applied. The same correction is assumed to apply at low temperatures. In all cases, the standard MAS, direct- or cross-polarisation sequences gave good  $^{19}\text{F}$  spectra with sufficient resolution to be able to use deconvolution to extract shift, intensity and linewidth parameters, so that CRAMPS operation was not necessary. Cross polarisation operation has the advantage of removing the small, broad probe background  $^{19}\text{F}$  signal (which is observed with direct polarisation), but as direct polarisation for fluorine can lead to a better signal-to-noise ratio, in a comparable time, this may be favoured when the background and desired signals are easily distinguished or where the latter is much greater than the former. Because of the resulting increased averaging of the strong homonuclear interactions, spinning at the higher spin rates (ca.12kHz) was found to give good resolution. Most spectra were recorded at ambient probe temperature, but this may be in excess of room temperature<sup>[27,28]</sup> by up to 15 degrees for the faster spin rates.

Fluorine-19 and phosphorus-31 spin-lattice relaxation times were measured using the Torchia sequence,<sup>[29]</sup> i.e. by  $^1\text{H}$   $^{19}\text{F}$  (or  $^{31}\text{P}$ ) CP followed by a 90  $^{19}\text{F}$  (or  $^{31}\text{P}$ ) pulse, a variable delay, and a 90  $^{19}\text{F}$  (or  $^{31}\text{P}$ ) read pulse. Proton decoupling was applied during acquisition but not during relaxation. In general, coupled spin systems will not yield single-exponential plots for relaxation times. However, the present measurements generally showed reasonably single-exponential curves. For proton spin-lattice relaxation times the pulse sequence used consisted of a 180 pulse on the proton channel followed by a variable delay, then a 90  $^1\text{H}$  pulse and contact to observe  $^{31}\text{P}$  spectra. The fitting of intensities in relaxation experiments was done within Chemagnetics Spinsight software. That for  $T_1$  used a three-parameter fit, taking into account the efficiency of the inversion. The number of data points recorded at each temperature was 1520 for  $T_1^H$ . For all  $T_1$  and  $T_1$  measurements for  $^{31}\text{P}$  and  $^1\text{H}$  12

data points were recorded, the maximum spin-lock time (an instrumental restriction) for the latter being 20 ms, which obviously limits the accuracy of measurement for long rotating frame relaxation times. Measurements of  $T_1$  and  $T_1$  generally have statistical errors of 28%, with the larger values being for longer relaxation times (where the end of the decay is not observed due to, for instance, limits on spin-lock time).

Spinning sideband analysis was carried out using an in-house program, ssb97,<sup>[30]</sup> based on the theory of Maricq and Waugh,<sup>[31]</sup> which includes the error analysis of Olivieri.<sup>[17]</sup> Between 5 and 11 peaks were fitted for the sideband manifolds analysed. The program anychi-x, used for calculating bandshapes of spin 1/2 spectra involving dipolar coupling to a quadrupolar nucleus, was written in BASIC and provided by Olivieri.<sup>[32]</sup>

**X-ray Diffraction:** The X-ray diffraction experiment was performed on a SMART 1K CCD area detector, using graphite-monochromated Mo-K radiation ( $\lambda = 0.71073 \text{ \AA}$ ). The structure was solved by direct methods and refined by full-matrix least-squares against  $F^2$  of all reflections, using SHELXL-97 programs.<sup>[33]</sup> *Crystal data:*  $\text{C}_{16}\text{H}_6\text{ClF}_{12}\text{P}$ ,  $M = 492.63$ ,  $T = 150\text{K}$ , triclinic, space group  $P1$  (No. 2),  $a = 7.949(1)$ ,  $b = 9.313(1)$ ,  $c = 12.369(1) \text{ \AA}$ ,  $\beta = 104.25(1)^\circ$ ,  $V = 90.49(1) \text{ \AA}^3$ ,  $U = 96.35(1) \text{ \AA}^3$ ,  $Z = 2$ ,  $D_c = 1.856 \text{ g cm}^{-3}$ ,  $\rho_{\text{calc}} = 0.43 \text{ mm}^{-1}$ , crystal size 0.36 0.34 0.34mm, 10579 reflections (4735 unique),  $R = 0.032$  [4253 data,  $I \geq 2(I)$ ],  $wR(F^2) = 0.086$ ,  $\text{max} = 0.58 \text{ e \AA}^{-3}$ .

Crystallographic data (excluding structure factors) for the structure(s) included in this paper have been deposited with the Cambridge Crystallographic Data Centre as supplementary publication no. CCDC-148986. Copies of the data can be obtained free of charge on application to CCDC, 12 Union Road, Cambridge CB2 1EZ, UK [Fax: (internat.) + 44-1223/336-033; Email: deposit@ccdc.cam.ac.uk].

## Acknowledgments

Two of us (L.A.C. and S.M.C.) thank the EPSRC for a studentship and another (M.D.R.) is grateful to the Department of Chemistry, University of Durham, for a studentship. We thank the EPSRC also for access both to the Durham-based research service in solid-state NMR (UDIRL) and to the Chemagnetics 600 system at Warwick. We acknowledge the receipt of research grants GR/L02906 and L24250 from the U.K. Engineering and Physical Sciences Research Council in support of this work. We are grateful to A. C. Olivieri for programming details and A. M. Kenwright and C. F. Heffernan for obtaining the solution-state  $^{13}\text{C}$  and  $^{19}\text{F}$  spectra.

- [1] K. B. Dillon, H. P. Goodwin, *J. Organomet. Chem.* **1992**, 429, 169171.
- [2] R. D. Chambers, K. B. Dillon, T. A. Straw, *J. Fluorine Chem.* **1992**, 56, 385388.
- [3] K. B. Dillon, H. P. Goodwin, *J. Organomet. Chem.* **1994**, 469, 125128.
- [4] K. B. Dillon, V. C. Gibson, L. J. Sequeira, *J. Chem. Soc., Chem. Commun.* **1995**, 24292430.
- [5] K. B. Dillon, V. C. Gibson, J. A. K. Howard, L. J. Sequeira, J. W. Yao, *Polyhedron* **1996**, 15, 41734177.
- [6] V. C. Gibson, C. Redshaw, L. J. Sequeira, K. B. Dillon, W. Clegg, M. R. J. Elsegood, *Chem. Commun.* **1996**, 21512152.
- [7] K. B. Dillon, V. C. Gibson, J. A. K. Howard, C. Redshaw, L. J. Sequeira, J. W. Yao, *J. Organomet. Chem.* **1997**, 528, 179183.
- [8] M. G. Davidson, K. B. Dillon, J. A. K. Howard, S. Lamb, M. D. Roden, *J. Organomet. Chem.* **1998**, 550, 481484.
- [9] R. K. Harris, A. C. Olivieri, *Prog. Nucl. Magn. Reson. Spectrosc.* **1992**, 24, 435456.



- [10] R. C. Crosby, J. F. Haw, *Macromolecules* **1987**, *20*, 23242326.
- [11] R. K. Harris, A. Root, *Mol. Phys.* **1989**, *66*, 9931013.
- [12] Chemagnetics Spinsight. Version 3.5.2. Otsuka Electronics (U. S. A.) Inc.
- [13] V. Mlynárik, *Prog. Nucl. Magn. Reson. Spectrosc.* **1986**, *18*, 277305 and references therein.
- [14] S. H. Alarcn, A. C. Olivieri, S. A. Carss, R. K. Harris, M. J. Zuriaga, G. A. Monti, *J. Magn. Reson. A* **1995**, *116*, 244250.
- [15] Gaussian 94 (Revision D.1) M. J. Frisch, G. W. Trucks, H. B. Schelegel, P. M. W. Gill, B. G. Johnson, M. A. Robb, J. R. Cheeseman, T. A. Keith, G. A. Petersson, J. A. Montgomery, K. Raghavachari, M. A. Al-Laham, V. G. Zakrzewski, J. V. Ortiz, J. B. Foresman, J. Cioslowski, B. B. Stefanov, A. Nanayakkara, M. Challacombe, C. Y. Peng, P. Y. Ayalla, W. Chen, M. W. Wong, J. L. Andres, E. S. Replogle, R. Gomperts, R. L. Martin, D. J. Fox, J. S. Binkley, D. J. Defrees, J. Baker, J. P. Stewart, M. Head-Gordon, C. Gonzalez, J. A. Pople, Gaussian, Inc., Pittsburgh PA, **1995**.
- [16] G. K. Semin, T. A. Babushkina, G. G. Yakobson, *Applications of NQR in Chemistry*, Khimiya, Leningrad, **1972**.
- [17] A. C. Olivieri, *J. Magn. Reson. A* **1996**, *123*, 207210.
- [18] S. Ando, R. K. Harris, S. A. Reinsberg, *J. Magn. Reson.* **1999**, *141*, 91103.
- [19] S. Ando, R. K. Harris, G. A. Monti, S. A. Reinsberg, *Magn. Reson. Chem.* **1999**, *37*, 709720.
- [20] P. Tekely, V. Gerardy, P. Palmas, D. Canet, A. Retournard, *Solid State NMR* **1995**, *4*, 361367.
- [21] S. J. Opella, M. H. Frey, *J. Am. Chem. Soc.* **1979**, *101*, 58545856.
- [22] F. H. Allen, *Acta Crystallogr., Sect. A* **1998**, *54*, 758771.
- [23] Yu. V. Zefirov, P. M. Zorkii, *Russ. Chem. Rev.* **1989**, *58*, 421440.
- [24] M. Franck, R. F. Hout Jr., W. J. Hehre, *J. Am. Chem. Soc.* **1984**, *106*, 563570.
- [25] A. N. Chernega, G. N. Koidan, A. P. Marchenko, *Zh. Strukt. Khim.* **1992**, *33*, 155.
- [26] S. A. Vierktter, *J. Magn. Reson. A* **1996**, *118*, 8493.
- [27] T. Bjornholm, H. J. Jakobsen, *J. Magn. Reson.* **1989**, *84*, 204211.
- [28] A.-R. Grimmer, A. Kretschmer, V. B. Cajipe, *Magn. Reson. Chem.* **1997**, *35*, 8690.
- [29] D. A. Torchia, *J. Magn. Reson.* **1978**, *30*, 613616.
- [30] J. R. Ascenso, L. H. Merwin, H.-P. Bai, J. C. Cherryman, unpublished work.
- [31] M. M. Maricq, J. S. Waugh, *J. Chem. Phys.* **1979**, *70*, 33003316.
- [32] A. C. Olivieri, personal communication.
- [33] G. M. Sheldrick, SHELXL-97 programs, University of Gottingen, **1997**.

Received November 23, 2000  
[I00447]